On-Surface Synthesis

International Edition: DOI: 10.1002/anie.201902784
German Edition: DOI: 10.1002/ange.201902784

Exploring a Route to Cyclic Acenes by On-Surface Synthesis

Fabian Schulz[+], Fátima García[+], Katharina Kaiser, Dolores Pérez, Enrique Guitián, Leo Gross, and Diego Peña**

Dedicated to Professor Sir J. Fraser Stoddart

Abstract: *A route to generate cyclacenes by on-surface synthesis is explored. We started by synthesizing two tetraepoxycyclacenes by sequences of Diels–Alder cycloadditions. Subsequently, these molecules were deposited onto Cu(111) and scanning-tunneling-microscopy(STM)-based atom manipulation was employed to dissociate the oxygen atoms. Atomic force microscopy (AFM) with CO-functionalized tips enabled the detailed characterization of the reaction products and revealed that, at most, two oxygens per molecule could be removed. Importantly, our experimental results suggest that the generation of cyclacenes by the described route might be possible for larger epoxycyclacenes.*

Carbon nanobelts (CNBs) are conjugated double-stranded macrocycles formed by the fusion of benzene rings comprising a closed loop.[1] For decades, the appealing curved structure of CNBs characterized by radially oriented p-orbitals has captivated chemists who have explored a large diversity of strategies for their preparation.[2] Finally, in 2017, Itami and co-workers succeeded in the first preparation and isolation of a CNB: a (6,6)-carbon nanotube (CNT) fragment formed by the angular fusion of 12 benzene rings.[3] This inspiring work renewed the long-standing interest in the synthesis of these polyarene belts.[4]

Cyclacenes,[5] the cyclic analogues of acenes formed by the flank-fusion of benzene rings, are particularly interesting CNBs and were first hypothesized in 1954 (Figure 1 a).[6]

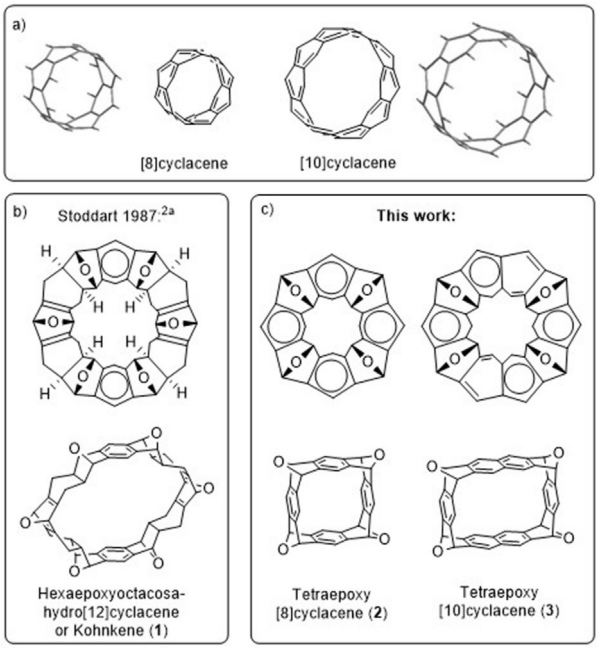

Figure 1. a) Structure of [8] and [10]cyclacene. b) Kohnkene (**1**) reported by Stoddart and co-workers.[2a] c) Tetraepoxycyclacenes **2** and **3** synthesized in this work.

Considered as the narrowest zig-zag CNTs, cyclacenes are expected to be highly reactive, not only due to the inherent strain of CNBs, but also based on their predicted open-shell character. In fact, theoretical calculations have suggested unusual electronic and magnetic properties for these curved aromatic molecules, which could be employed to develop novel organic materials.[7] Although several groups have described elegant strategies to attempt the preparation of cyclacenes by solution chemistry, this challenging goal remains elusive. In a seminal work, Stoddart and co-workers used a sequence of successive Diels–Alder reactions to build hexaepoxyoctacosahydro[12]cyclacene (**1**, Figure 1 b).[2a–c] Unfortunately, attempts to aromatize **1** by deoxygenation/dehydration protocols did not yield the elusive [12]cyclacene but a partially hydrogenated derivative.[2b]

Recently, some of us have developed a synthetic methodology based on aryne cycloadditions for the preparation of epoxyacenes, which were used as precursors for the on-surface generation of large acenes.[8] In particular, through successive Diels–Alder reactions between arynes and furan derivatives, we prepared tetraepoxydecacenes, which yielded decacene by on-surface deoxygenation.[9] Inspired by the

[*] Dr. F. García,[+] Prof. Dr. D. Pérez, Prof. Dr. E. Guitián, Prof. Dr. D. Peña
Centro de Investigación en Química Biolóxica e Materiais Moleculares (CIQUS) and Departamento de Química Orgánica
Universidade de Santiago de Compostela
15782-Santiago de Compostela (Spain)
E-mail: diego.pena@usc.es
Dr. F. Schulz,[+] K. Kaiser, Dr. L. Gross
IBM Research—Zurich
8803 Rüschlikon (Switzerland)
E-mail: LGR@zurich.ibm.com
[+] These authors contributed equally to this work.
Supporting information and the ORCID identification number(s) for the author(s) of this article can be found under: https://doi.org/10.1002/anie.201902784.

synthesis of **1**, we speculated about the possibility of using our aryne methodology to obtain epoxycyclacenes, which could lead to cyclacenes by deoxygenation. Herein, we describe the synthesis of tetraepoxycyclacenes **2** and **3** (Figure 1c) and their on-surface characterization by atomic force microscopy (AFM) and scanning tunneling microscopy (STM). Furthermore, we explore the on-surface generation of [8]- and [10]cyclacene from **2** and **3**, respectively. Although these cyclacenes were not detected on-surface, we found that partial deoxygenation is possible by atom manipulation, indicating that for larger ring sizes, this approach, which combines solution and surface synthesis, might be feasible.

Tetraepoxycyclacenes **2** and **3** are shape-persistent macrocycles with D_{4h} and D_{2h} symmetry, respectively. Scheme 1a shows the retrosynthetic analysis we followed to build both molecules. Based on the high symmetry of square-shaped tetraepoxy[8]cyclacene **2**, we envisioned that it could be synthesized in one step by a cascade of four Diels–Alder cycloadditions involving a single bifunctional AB-type monomer, a strategy previously employed by Schlüter and coworkers to prepare CNB precursors.[2g] In particular, we speculated about the possible cyclotetramerization of the highly reactive 5,6-didehydroisobenzofuran (**4**), which contains both a diene (furan) and a dienophile (aryne) in the same molecule (Scheme 1a).[10] In contrast, for the synthesis of rectangularly-shaped compound, **3** we decided to use two different monomers, a bisdiene and a bisdienophile, similarly to the strategies used by the groups of Stoddart[2a] and Cory.[2d–e] In this case, we envisioned a two-step synthesis via the double Diels–Alder reaction of bisaryne **5** with benzodifuran equivalent **6**. In general, tetraepoxy[10]cyclacene **3** could be built by the reaction of two molecules of bisfuranoid **6** with two molecules of bisnaphthalyne **7** by a sequence of four Diels–Alder cycloadditions.

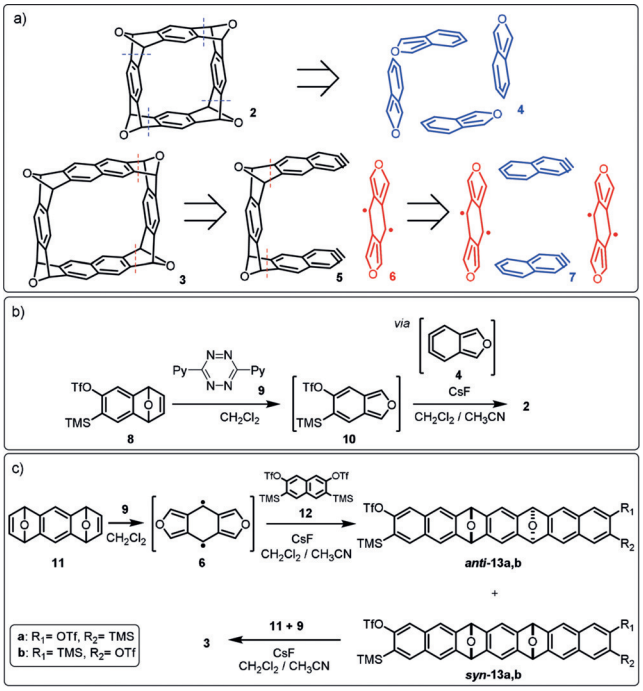

Scheme 1. a) Retrosynthesis and b), c) synthetic routes used for the preparation of tetraepoxycyclacenes **2** (b) and **3** (c).

We first explored the generation and cyclotetramerization of 5,6-didehydroisobenzofuran (**4**) to obtain macrocycle **2** in one pot. With this idea in mind, we treated triflate **8** with 3,6-di-2-pyridyl-1,2,4,5-tetrazine (**9**) to induce a formal acetylene extrusion and generate the highly reactive isobenzofuran **10** (Scheme 1b). Then, under high-dilution conditions, CsF was added to form **4**, which underwent cyclotetramerization to afford tetraepoxy[8]cyclacene **2** as a white solid in 5% yield. Mass spectrometry of the reaction mixture suggested that no other macrocyclization product was formed in the reaction.[11]

With the idea of approaching larger CNBs, we decided to prepare tetraepoxy[10]cyclacene **3**. First, diepoxyanthracene **11** was reacted with tetrazine **9**, generating the corresponding bisfuranoid **6** which reacted in situ with two equivalents of bistriflate **12** in the presence of CsF (Scheme 1c). This reaction generated the bistriflates **13** as a mixture of four isomers (that is, regioisomers **a** and **b** and diastereomers ***anti*** and ***syn***) in 43% yield. It should be mentioned that only ***syn*-13a,b**, precursors of bisaryne **5**, could afford compound **3** (Scheme 1a). Therefore, after separation of ***syn*-13a,b** from the reaction mixture, its treatment with intermediate **6** in the presence of CsF lead to the formation of tetraepoxy[10]cyclacene **3** as a yellow solid in 15% yield.

To confirm the structure of both epoxycyclacenes **2** and **3**, we performed X-ray diffraction analysis. Slow evaporation of a CH_2Cl_2 solution of **2** yielded colourless needles, while slow diffusion of CH_3CN into a $CHCl_3$ solution of compound **3** produced pale yellow crystals, which were suitable for X-ray diffraction analysis (Figure 2). The larger inner cavity of macrocycle **3**, in comparison with **2**, allows hosting the methyl group of a CH_3CN molecule inside its cavity, suggesting that these compounds may be useful to encapsulate small molecules.

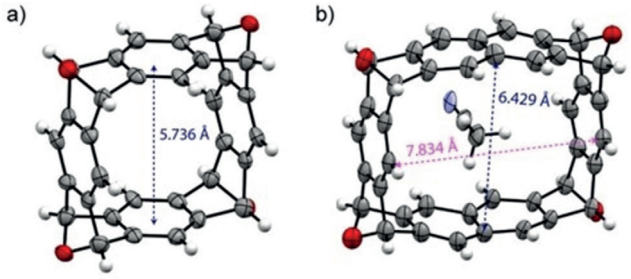

Figure 2. X-ray crystal structure of tetraepoxycyclacenes **2** (a) and **3** (b). A molecule of CH_3CN is found inside the molecular cavity of compound **3**. Grey, carbon; white, hydrogen; red, oxygen; blue, nitrogen.

Next, we aimed for the on-surface deoxygenation of compounds **2** and **3** in an attempt to generate the corresponding cyclacenes, an approach that had been successful for the creation of several long planar acenes.[8,9] We employed STM and AFM with CO-functionalized tips[12] for the characterization of **2** and **3** on the surface and for the analysis of their reaction products (for details on the scanning probe measure-

ments, see the Methods section in the Supporting Information).[13,14]

Figure 3a shows an STM image of a single molecule of **2** after deposition of a sub-monolayer coverage onto a Cu(111) substrate held at 10 K. Corresponding AFM images acquired with a CO-functionalized tip are shown in Figure 3b,c. They reveal a central ring and two additional protrusions at opposing sides of the ring. We attribute the former to one of the four benzene units of **2** and the latter to two oxygens. This indicates that the molecule adsorbs with one aromatic ring parallel to the surface and the ring on the opposite side is imaged by the AFM. We attempted the deoxygenation of compound **2** using voltage pulses from the tip. However, the identification of the reaction product is difficult in this upstanding conformation because only a small fraction of the molecule can be resolved in AFM (for an example, see Figure S1 in the Supporting Information). The reaction products could be better characterized in an adsorption position where a larger fraction of the molecule can be imaged, which was achieved by thermal annealing.

Figure 3d is an STM image of a self-assembled island of **2** after annealing the sample to 370 K, and the corresponding AFM images are depicted in Figure 3e,f. Now, the molecules appear four-fold symmetric and they are packed in a square lattice (Figure 3i). Figure 3g highlights the details of the AFM

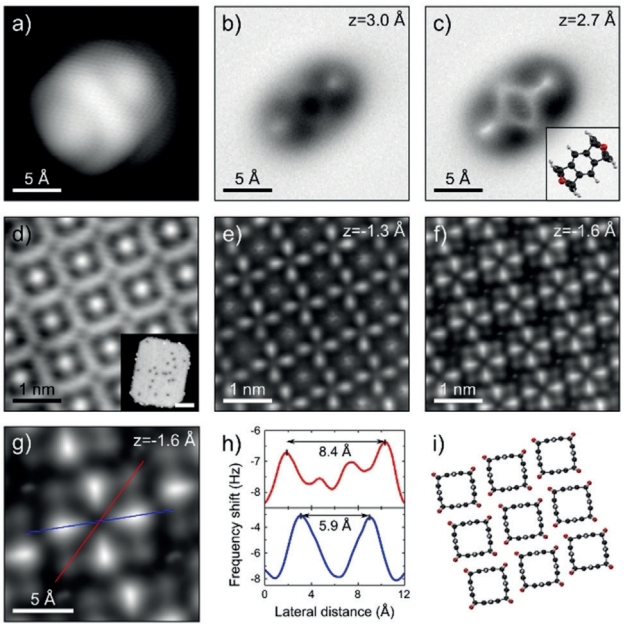

Figure 3. a) Constant-current STM image ($V = 0.4$ V, $I = 0.5$ pA) of **2** after low-temperature deposition onto Cu(111). b),c) Constant-height AFM images of the same molecule as in (a), acquired with a CO-functionalized tip at two different tip heights *z*. Inset: Structural model of **2**, indicating the molecular orientation. d) STM image ($V = 0.2$ V, $I = 1.0$ pA) of a two-dimensional self-assembled island after annealing **2** on Cu(111) to 370 K. Inset: STM overview image ($V = 0.2$ V, $I = 1.0$ pA) of a typical self-assembled island. Scale bar is 10 nm. e),f) Constant-height AFM images of the same area as in (d), acquired at two different tip heights *z*. g) Zoomed-in AFM image of one of the molecules within the self-assembled island. h) Color-coded line profiles taken along the lines shown in (g). i) Proposed structure of self-assembled islands of **2** on Cu(111).

contrast corresponding to the individual molecules. They are imaged as a square with four bright protrusions located at its sides and four darker protrusions at its corners. Line profiles along the two kinds of protrusions are depicted in Figure 3h. The distance between two brighter protrusions is approx. 5.9 Å and shows good agreement with the distance between the hydrogen atoms connected to opposite aromatic rings in the density-functional-theory(DFT)-optimized structure of **2** of 5.66 Å. This value is also in good agreement with the size of the molecular cavity obtained from the X-ray diffraction measurements of 5.74 Å (Figure 2a). Similarly, the distance between two darker protrusions of approximately 8.4 Å is in good agreement with the theoretical distance of 8.48 Å between the hydrogen atoms connected to opposite epoxy groups. Thus, within the self-assembled islands, **2** adsorbs in a lying conformation with the planes of the aromatic rings perpendicular to the surface. The brightness of the hydrogen atoms in the AFM images is directly related to the hybridization state of the connecting carbon atoms: The four hydrogen atoms connected to the sp^2-hybridized carbon atoms of the benzene units are closer to the tip because they point nearly straight up with respect to the surface plane, while the hydrogen atoms connected to the sp^3-hybridized carbon atoms of the epoxy groups are slightly tilted away from the molecular cavity.

The conversion from upstanding single molecules after low-temperature deposition to lying molecules within the self-assembled islands after annealing is most likely driven by intermolecular van-der-Waals (vdW) or π–π interactions.[15,16] After low-temperature deposition, molecule–surface interactions dominate and favor an adsorption position with one of the benzene units parallel to the Cu(111) surface. Upon supplying thermal energy, molecule–molecule interactions become important and the molecules maximize intermolecular vdW/π–π interactions by assembling in a way such that benzene units of neighboring molecules face each other.

We observed a similar change in the adsorption for **3**, as depicted in Figure 4. Upon low-temperature deposition of **3** onto Cu(111), we find molecules in two different adsorption geometries, whose main difference in STM images is their different apparent height at low voltages (Figure 4a). The AFM measurements (Figure 4b,c) reveal that the molecule with the higher feature is adsorbed with a benzene unit parallel to the Cu(111) surface, while the other is adsorbed with the naphthalene unit parallel to the surface.

Figure 4d,e shows STM and AFM images, respectively, of the molecular islands that are formed after annealing the sample to 420 K. In the AFM image, the upward-pointing hydrogen atoms give rise to six prominent protrusions and the rectangular cavity of the molecules can be observed. The proposed self-assembled structure is shown in Figure 4f and consists of molecules arranged in a rectangular lattice.

The lying adsorption geometry allows for an easier evaluation of whether tip-induced deoxygenation was successful, as demonstrated in the following. Figure 5a shows an AFM image of a self-assembled island of **3** after the lower part of the area was imaged by STM at $V = 3$ V. The contrast of most of the molecules has changed, and two examples of such molecules are marked by a red and a blue square.

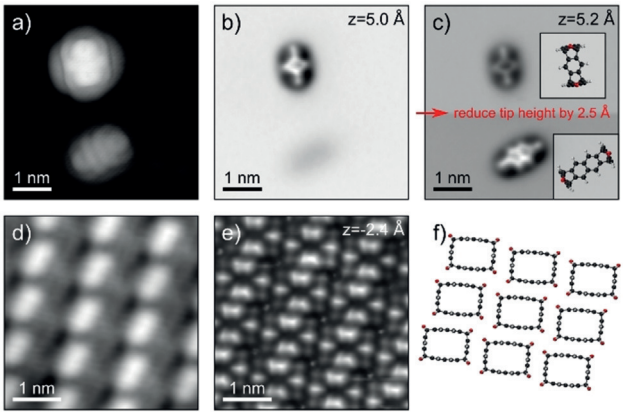

Figure 4. a) STM image ($V = 0.4$ V, $I = 0.5$ pA) of **3** after low-temperature deposition onto Cu(111), showing the two different adsorption geometries observed. b), c) Corresponding AFM images, recorded at different tip heights z. Insets: Structural models of **3**, indicating the different molecular orientations. d) STM image ($V = 0.4$ V, $I = 1.0$ pA) of a self-assembled island after annealing the sample to 420 K. e) Corresponding AFM image. f) Proposed self-assembled structure of **3** on Cu(111).

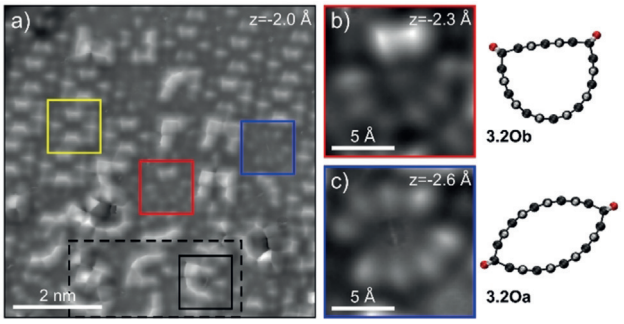

Figure 5. a) AFM image of a self-assembled island of **3** acquired after scanning the lower part of the imaged area (dashed box) at a sample voltage of 3 V. $V = 0.4$ V, $I = 1.0$ pA. b), c) Zoomed-in AFM images of two molecules as indicated by the colored boxes in panel (a) along with models of the proposed molecular structures. For comparison, a pristine molecule (yellow box) and a molecule with one dissociated oxygen (black box) are highlighted in panel (a) as well.

Zoomed-in AFM images of each molecule are shown in Figure 5b, c. For comparison, a pristine molecule is marked by a yellow square in Figure 5a, showing the same contrast as the molecules in Figure 4e. Each deoxygenation step changes the shape and symmetry of the molecular cavity. Furthermore, it alters the hybridization state of the carbon atoms of the corresponding epoxy group from sp^3 to sp^2. That, in turn, increases the height of the associated protruding hydrogen atom and thus its brightness in the AFM images, as discussed above. We can utilize this knowledge to assign the number of remaining oxygens for the molecules shown in Figure 5b, c. The molecule in the AFM image in Figure 5b is D-shaped, and the dark hydrogens at the corners suggest that they are connected to sp^3-hybridized carbon atoms of the epoxy group. This leads to the structure **3.2Ob** (Figure 5b) with two neighboring epoxy groups being deoxygenated and the other two still intact. This structure presents a highly strained bent hexacene moiety, suggesting that the on-surface approach to cyclacenes is feasible. Similarly, the molecule in Figure 5c also has two dark hydrogens left, indicating sp^3-hybridized carbon atoms below them. However, here they are located on opposite sides, giving the molecular cavity an oval shape. The corresponding molecular structure (**3.2Oa**) has two opposite epoxy groups deoxygenated, but the remaining two are still intact. We find a larger fraction of **3.2Oa** than of **3.2Ob**, in agreement with DFT calculations (for statistics and DFT results, see Figure S3 and Figure S4 in the Supporting Information).

We were not able to identify any molecules with less than two oxygen atoms, despite further manipulation attempts at voltages ranging from 2.5 to 3.4 V and currents of up to 30 pA (at 3.4 V). Manipulation attempts at increasingly harsher current and voltage parameters usually lead to molecular degradation, up to the point where the structure could not be identified anymore. We did not find a significant difference in the manipulation outcome between scanning the molecular island at large bias or applying single voltage pulses with the tip position fixed above one molecule. The latter approach also resulted in other molecules in the surrounding area being deoxygenated or altered otherwise. This indicates that the deoxygenation mechanism is not very local, but could be mediated by surface-state electrons.[17,18] Otherwise, the Cu(111) surface probably plays a smaller role compared to the on-surface deoxygenation of linear epoxyacenes.[8] All oxygen atoms are elevated from the Cu surface in the lying adsorption conformation. Nevertheless, the adsorption might lower the energy barrier for the deoxygenation reaction for all oxygen atoms, for example by partial charge transfer between molecule and surface or through interactions via the hydrogen atoms. We have carried out analogous manipulation experiments for tetraepoxy[8]cyclacene **2** and the results are very similar. Briefly, also for **2**, we were only able to dissociate two oxygens at most, generating the oval-shaped diepoxy-[8]cyclacene (for examples, see Figure S2 in the Supporting Information).

To understand the experimental observations, we estimated the energy balance associated with each deoxygenation reaction by DFT calculations (for details on the calculations and the full results, see the Methods section and Figure S4 in the Supporting Information). According to these calculations, the energy cost for the first deoxygenation of **2** and **3** (3.185 eV and 3.234 eV, respectively) is moderate compared to the deoxygenation of the oval-shaped diepoxy[8]cyclacene and diepoxy[10]cyclacene (4.176 eV and 4.032 eV, respectively). This provides an explanation why we were not able to further deoxygenate the diepoxycyclacenes in a controlled fashion. Because the energy for the third deoxygenation decreases from **2** to **3**, we also calculated the corresponding value for diepoxy[12]cyclacene, which led to 3.830 eV (see Figure S4 in the Supporting Information). These values can be intuitively understood by considering how the curvature of the macrocycle and thus its internal strain changes. Notably, these calculations suggest that further deoxygenation might be possible for larger diepoxycyclacenes.

In summary, we synthesized tetraepoxycyclacenes with 8 and 10 units in an extremely simple manner and succeeded in

their partial deoxygenation by STM/AFM-based atom manipulation. Work is in progress to attempt our on-surface synthesis route for larger derivatives, which may allow for the dissociation of all oxygens, thereby generating the thus far elusive cyclacenes. Bearing in mind the unusual electronic and magnetic properties predicted for these curved aromatic molecules, our approach could pave the way to the development of a new class of organic materials.

Acknowledgements

We thank R. Allenspach, N. Moll and M. Melle-Franco for comments and discussions. We acknowledge financial support by the ERC Consolidator Grant AMSEL (682144), the Agencia Estatal de Investigación (MAT2016-78293-C6-3-R and CTQ2016-78157-R), Xunta de Galicia (Centro singular de investigación de Galicia, accreditation 2016-2019, ED431G/09), and the Fondo Europeo de Desarrollo Regional (FEDER). F.G. acknowledges the Juan de la Cierva Incorporación 2017 program.

Conflict of interest

The authors declare no conflict of interest.

Keywords: atomic force microscopy · arynes · carbon nanobelts · cyclacenes · cycloadditions · scanning tunneling microscopy

How to cite: *Angew. Chem. Int. Ed.* **2019**, *58*, 9038 – 9042
Angew. Chem. **2019**, *131*, 9136 – 9140

[1] a) D. Eisenberg, R. Shenhar, M. Rabinovitz, *Chem. Soc. Rev.* **2010**, *39*, 2879 – 2890; b) K. Tahara, Y. Tobe, *Chem. Rev.* **2006**, *106*, 5274 – 5290; c) L. T. Scott, *Angew. Chem. Int. Ed.* **2003**, *42*, 4133 – 4135; *Angew. Chem.* **2003**, *115*, 4265 – 4267.

[2] a) F. H. Kohnke, A. M. Z. Slawin, J. F. Stoddart, D. J. Williams, *Angew. Chem. Int. Ed. Engl.* **1987**, *26*, 892 – 894; *Angew. Chem.* **1987**, *99*, 941 – 943; b) P. R. Ashton, G. R. Brown, N. S. Isaacs, D. Giuffrida, F. H. Kohnke, J. P. Mathias, A. M. Z. Slawin, D. R. Smith, J. F. Stoddart, D. J. Williams, *J. Am. Chem. Soc.* **1992**, *114*, 6330 – 6353; c) P. R. Ashton, U. Girreser, D. Giuffrida, F. H. Kohnke, J. P. Mathias, F. M. Raymo, A. M. Z. Slawin, J. F. Stoddart, D. J. Williams, *J. Am. Chem. Soc.* **1993**, *115*, 5422 – 5429; d) R. M. Cory, C. L. McPhail, A. J. Dikmans, J. J. Vittal, *Tetrahedron Lett.* **1996**, *37*, 1983 – 1986; e) R. M. Cory, C. L. McPhail, *Tetrahedron Lett.* **1996**, *37*, 1987 – 1990; f) M. Standera, D. Schlüter, in *Fragments of Fullerenes and Carbon Nanotubes* (Ed.: L. T. S. M. A. Petrukhina), Wiley, Hoboken, **2011**, pp. 343 – 366; g) W. D. Neudorff, D. Lentz, M. Anibarro, A. D. Schlüter, *Chem. Eur. J.* **2003**, *9*, 2745 – 2757; h) F. Vögtle, *Top. Curr. Chem.* **1983**, *115*, 157; i) F. Vögtle, A. Schröder, D. Karbach, *Angew. Chem. Int. Ed. Engl.* **1991**, *30*, 575 – 577; *Angew. Chem.* **1991**, *103*, 582 – 584; j) T. Yao, H. Yu, R. J. Vermeij, G. J. Bodwell, *Pure Appl. Chem.* **2008**, *80*, 533 – 546.

[3] G. Povie, Y. Segawa, T. Nishihara, Y. Miyauchi, K. Itami, *Science* **2017**, *356*, 172 – 175.

[4] a) J. S. Siegel, *Science* **2017**, *356*, 135 – 136; b) G. Povie, Y. Segawa, T. Nishihara, Y. Miyauchi, K. Itami, *J. Am. Chem. Soc.* **2018**, *140*, 10054 – 10059.

[5] R. Gleiter, B. Esser, S. C. Kornmayer, *Acc. Chem. Res.* **2009**, *42*, 1108 – 1116.

[6] E. Heilbronner, *Helv. Chim. Acta* **1954**, *37*, 921 – 935.

[7] a) H. S. Choi, K. S. Kim, *Angew. Chem. Int. Ed.* **1999**, *38*, 2256 – 2258; *Angew. Chem.* **1999**, *111*, 2400 – 2402; b) Z. Chen, D. Jiang, X. Lu, H. F. Bettinger, S. Dai, P. von Ragué Schleyer, K. N. Houk, *Org. Lett.* **2007**, *9*, 5449 – 5452.

[8] J. Krüger, N. Pavliček, J. M. Alonso, D. Pérez, E. Guitián, T. Lehmann, G. Cuniberti, A. Gourdon, G. Meyer, L. Gross, F. Moresco, D. Peña, *ACS Nano* **2016**, *10*, 4538 – 4542.

[9] J. Krüger, F. García, F. Eisenhut, D. Skidin, J. M. Alonso, E. Guitián, D. Pérez, G. Cuniberti, F. Moresco, D. Peña, *Angew. Chem. Int. Ed.* **2017**, *56*, 11945 – 11948; *Angew. Chem.* **2017**, *129*, 12107 – 12110.

[10] For the recent synthetic use of a substituted didehydroisobenzofuran for the construction of polycyclic structures, see: S. Matsuoka, S. Jung, K. Miyakawa, Y. Chuda, R. Sugimoto, T. Hamura, *Chem. Eur. J.* **2018**, *24*, 18886 – 18889.

[11] See the Supporting Information for details.

[12] L. Gross, F. Mohn, N. Moll, P. Liljeroth, G. Meyer, *Science* **2009**, *325*, 1110 – 1114.

[13] D. G. de Oteyza, P. Gorman, Y.-C. Chen, S. Wickenburg, A. Riss, D. J. Mowbray, G. Etkin, Z. Pedramrazi, H.-Z. Tsai, A. Rubio, M. F. Crommie, F. R. Fischer, *Science* **2013**, *340*, 1434 – 1437.

[14] N. Pavliček, B. Schuler, S. Collazos, N. Moll, D. Pérez, E. Guitián, G. Meyer, D. Peña, L. Gross, *Nat. Chem.* **2015**, *7*, 623 – 628.

[15] Q. S. Stöckl, Y.-C. Hsieh, A. Mairena, Y.-T. Wu, K.-H. Ernst, *J. Am. Chem. Soc.* **2016**, *138*, 6111 – 6114.

[16] C. A. Hunter, J. K. M. Sanders, *J. Am. Chem. Soc.* **1990**, *112*, 5525 – 5534.

[17] V. Schendel, B. Borca, I. Pentegov, T. Michnowicz, U. Kraft, H. Klauk, P. Wahl, U. Schlickum, K. Kern, *Nano Lett.* **2016**, *16*, 93 – 97.

[18] J. N. Ladenthin, L. Grill, S. Gawinkowski, S. Liu, J. Waluk, T. Kumagai, *ACS Nano* **2015**, *9*, 7287 – 7295.

Manuscript received: March 5, 2019
Revised manuscript received: April 12, 2019
Accepted manuscript online: April 26, 2019
Version of record online: May 22, 2019

